Seminars in Cell and Developmental Biology xxx (xxxx) xxx–xxx

Contents lists available at ScienceDirect

Seminars in Cell & Developmental Biology

journal homepage: www.elsevier.com/locate/semcdb

Clustered cell migration: Modeling the model system of Drosophila border cells

Bradford E. Peercy[a,*], Michelle Starz-Gaiano[b]

[a] Department of Mathematics and Statistics, UMBC, Baltimore, MD 21250, United States
[b] Department of Biological Sciences, UMBC, Baltimore, MD 21250, United States

ARTICLE INFO

Keywords:
Border cells
Mathematical model
Clustered cell migration
Drosophila genetics

ABSTRACT

In diverse developmental contexts, certain cells must migrate to fulfill their roles. Many questions remain unanswered about the genetic and physical properties that govern cell migration. While the simplest case of a single cell moving alone has been well-studied, additional complexities arise in considering how cohorts of cells move together. Significant differences exist between models of collectively migrating cells. We explore the experimental model of migratory border cell clusters in *Drosophila melanogaster* egg chambers, which are amenable to direct observation and precise genetic manipulations. This system involves two special characteristics that are worthy of attention: border cell clusters contain a limited number of both migratory and non-migratory cells that require coordination, and they navigate through a heterogeneous three-dimensional microenvironment. First, we review how clusters of motile border cells are specified and guided in their migration by chemical signals and the physical impact of adjacent tissue interactions. In the second part, we examine questions around the 3D structure of the motile cluster and surrounding microenvironment in understanding the limits to cluster size and speed of movement through the egg chamber. Mathematical models have identified sufficient gene regulatory networks for specification, the key forces that capture emergent behaviors observed *in vivo*, the minimal regulatory topologies for signaling, and the distribution of key signaling cues that direct cell behaviors. This interdisciplinary approach to studying border cells is likely to reveal governing principles that apply to different types of cell migration events.

1. Introduction

Multicellular movement through structurally complex environments occurs during normal animal development as well as in pathologies including immune diseases and metastasis. The biological system of the *Drosophila melanogaster* egg chamber has become a popular *in vivo* platform to study the specific case of clustered cell migration because it is amenable to genetic manipulation and live imaging [1–4]. Moreover, the conservation of genetic and molecular mechanics of cell migration with other animals, including humans, makes Drosophila a powerful 'model' system for discovery and exploration of the genetic regulation behind cell migration.

Among multiple cell types that migrate during fly development, the ovarian border cells have emerged as an interesting case to study the coordinated movements of a small group of cells (reviewed in [1,5–7]). Within the adult fly ovary, at the anterior end of a developing egg chamber, a small set of somatic cells– named the border cells – are induced to a migratory fate by two signaling cells – the polar cells. The border cell cluster, comprising both cell types, responds to chemoattractants and moves between a sea of crowding germline cells toward the oocyte border (Fig. 1). This event is required for formation of a fertilizable egg. The advent of methods to image border cells in living egg chambers [8–11] has improved our understanding of the process, but some curious behaviors exhibited by these dynamic cells have also opened up many more questions. The complexities of this system stem from the border cells' abilities to interpret biochemical and mechanical cues, integrate intracellular and extracellular signaling, and translate local spatial information into global cellular relocation all amidst an enlarging egg chamber rescaling the domain. Because of this complexity, these puzzles are challenging to answer through genetic manipulation alone. Applying a mathematical framework to many of these aspects has proven important and useful.

In this article, we focus on questions that have motivated the study of the Drosophila border cells and the accompanying mathematical formulations, solutions, and predictions suggested by biological and mathematical methods. First, in Section 2, we review studies on how

* Corresponding author.
E-mail address: bpeercy@umbc.edu (B.E. Peercy).

https://doi.org/10.1016/j.semcdb.2019.11.010
Received 1 July 2019; Received in revised form 11 November 2019; Accepted 15 November 2019

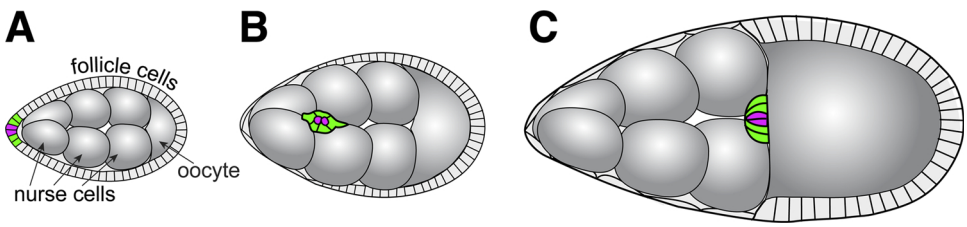

Fig. 1. Border cell migration in Drosophila egg chambers. Egg chambers consist of an outer, somatic follicle cell layer, within which the anterior polar cells (magenta) induce specification of border cells (green). Interiorly, fifteen nurse cells and one oocyte develop over a series of fourteen stages. A) At stage 8, the motile cells are specified. (Staging according to [13]). B) At stage 9, the border cells move out of the epithelium and between nurse cells, toward the oocyte. C) At stage 10, the border cells arrive at the oocyte.

some somatic follicle cells are activated in response to chemical cues, which is required for them to become motile. We also examine the effects of the local tissue environment on cellular signaling and cluster movement. In Section 3, we discuss the relationship between forces and velocity after the cells start to migrate, consider the predicted constraints on motile cluster size, and explore the minimal signaling topologies to account for migratory behavior.

2. Motile cell specification in the Drosophila ovary

The border cells arise within a layer of somatic, follicle cells that surround the oocyte and its sister cells, called nurse cells, during mid-oogenesis (Fig. 1 and reviewed in [1,3,5–7,12]). Within this epithelial layer, cells are stable, tightly connected to their neighbors, and encased on the outer surface by a basement membrane. Therefore, for the border cells to break out of the epithelium and become migratory, they must change many of their physical characteristics, undergoing a partial epithelial to mesenchymal transition (EMT). The transition is partial since the cells preserve some epithelial characteristics, such as apico-basal polarity.

Genetic analysis from several laboratories revealed that the Janus Kinase and Signal Transducer and Activator of Transcription (Jak/STAT) signaling pathway is necessary and sufficient for the acquisition of follicle cell motility [14–18]. This signaling is well-conserved from flies to mammals, and evidence from an array of organisms has elucidated the cascade of core components in this pathway (Reviewed in [19–22]). Jak/STAT signaling is activated in follicle cells by the protein Unpaired (Upd), which is secreted from the polar cells [18,23–27]. Upd binds a cell surface receptor dimer (Domeless in flies, interleukin receptors in humans), which induces activation of its associated Jaks, and this complex in turn recruits and phosphorylates STAT. Phospho-STATs dimerize to an active form, and the dimers enter the nucleus and turn on transcription of target genes. In particular, STAT activity promotes expression of the homolog of the human CCAAT/Enhancer Binding Protein transcription factor, encoded in flies by *slow border cells (slbo),* which is necessary for motile border cell fate [16,28,29]. Upd elicits at least two different outputs depending on concentration, such that cells close to the polar cells become border cells while those further away have lower levels of STAT signaling and stay in the epithelium [18,29,30].

2.1. Should I stay or should I go now? Mathematical models support a minimal signaling feedback switch mechanism of cell fate determination

While many anterior follicle cells activate STAT, only about six maintain it at sufficient levels to become motile [29]. Molecularly, what could account for specifying the right number of migratory epithelial cells while preventing this signal from being active in neighboring, stationary cells? An explanation started to emerge with the characterization of *apontic (apt)* mutants. Loss of function mutants for *apt* harbor additional migratory cells, mimicking over-activation of STAT signaling [29] – suggesting that Apt acts as a negative regulator of STAT signaling and that it is needed to specify the optimal number of motile cells. However, like for *slbo*, STAT signaling activates *apontic (apt)* gene expression, so it was initially confusing how these seemingly opposing signals would resolve to induce an appropriate number of migratory cells. Genetic analysis demonstrated that the *apt* and *slbo* genes respond differently to different levels of STAT activation, resulting in a gradient of Slbo expression but relatively even levels of Apt protein across the follicular epithelium [29]. Further, it was shown that the pro-migratory Slbo and anti-migratory Apt act to cross-repress one another, which suggested that these signals could mediate a molecular switch between stationary and migratory fates (Fig. 2A). Initial mathematical modeling by Meinhardt [29–31] (see Box 1) showed that the activation of motile cell fate due to the STAT/Slbo pathway "winning" could arise due to coexistence of two stable steady states (bistability) often associated with switch-like behavior. This phenomenological model utilized general positive and negative feedback functional forms, demonstrating that the Apt/Slbo/STAT system is sufficient to explain the behavior.

A comparison of these early models highlights their key features. In Starz-Gaiano et al. [28], a partial differential equation model captured secretion, uptake and diffusion of Upd in a one-dimensional domain. The cells respond to the level of Upd they experience by proportionally activating Jak/STAT signaling, which in turn activates Apt and Slbo to differing extents based on their responsiveness to STAT activity and cross-repression (Fig. 2A-B and Box 1). Several factors beyond the baseline decay of Jak/STAT proteins are used to inhibit pathway activation including secretion level of Upd, Jak/STAT activation itself, and the presence of Slbo to dampen the signaling inhibition by Apt. The threshold between motility (higher Slbo) and non-motility (higher Apt) becomes a quantitative choice of parameters, but there is an inherent potential for underlying bistability [31] (Box 1, left). In this model, Slbo is produced by Jak/STAT-mediated transcription, is inhibited cooperatively only by Apt, and is subject to baseline degradation. In contrast, Apt levels depend on its baseline production (due to another factor, Eyes absent (Eya)) plus Jak/STAT-mediated production, which is inhibited both cooperatively by itself and through Slbo action, and on degradation as a counterbalance to production. The result is a model which, for a graded distribution of Upd, creates a definitive fate designation at each cell. In the Yoon et al. [30] model, a similar result is achieved but it incorporates additional regulation by *miR-279*, a microRNA that is activated by Apt and inhibits *Stat* mRNA directly, and another Jak/STAT-activated protein, Ken and Barbie (Ken), which functions to lower *miR-279* levels in motile cells (Box 1, right). Cooperativity of components between the Yoon et al. [30] and Starz-Gaiano et al. [29,31] models varies, but the nonlinear components are still critical to maintain multiple steady states of bistability (Box 1).

While the models from Starz-Gaiano et al. [29,31] and Yoon et al. [30] accurately captured bistable behavior, it is hard to incorporate newly identified regulators into this system. Thus, we sought to create a more mechanistic model. In an attempt to relate the Meinhardt-derived models to mechanistic reactions, including probabilities of transcriptional activation, rates of transcript production and turnover, and protein production and turnover for Apt, Slbo, and STAT, our students Ge and Stonko [32] developed a fifteen variable ordinary differential equation model downstream of the Upd spatial distribution, which

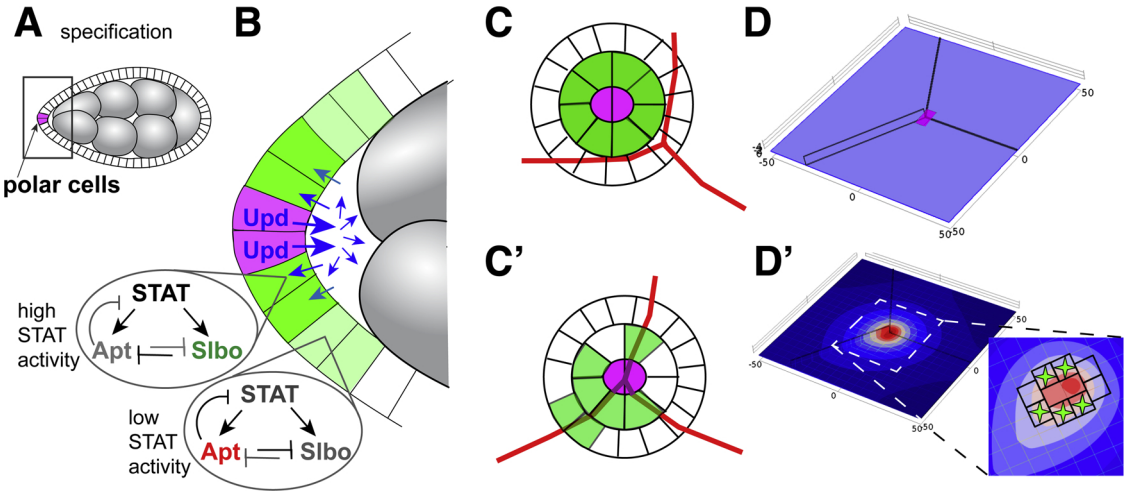

Fig. 2. High levels of STAT signaling induce border cell fate, which can depend on tissue structure. A) At stage 8 of egg chamber development, anterior polar cells (magenta) secrete instructive cues to nearby epithelial cells and are juxtaposed by large germline cells (gray). **B)** Polar cells release the cytokine Upd, which diffuses in the adjacent domain. Cells that uptake high levels of Upd activate STAT signaling highly (green), activating Slbo expression and promoting motility. Cells in contact with less Upd activate STAT to a lesser extent (light green), and this lower signaling is switched off through a bistable circuit that includes the feedback regulator Apt. C and C') An end on-view of the anterior part of the egg chamber, showing the Y-shaped clefts (red) created by three juxtaposed germline cells below the epithelium. In C, border cells are specified in a radially symmetric pattern. In C', the clefts pool the Upd activator and influence which epithelial cells become motile. D) A model of the Y-shaped cleft domains with magenta polar cells in the underlying blue plane. D') Results of a simulation showing different levels of Upd distribution from red (high) to blue (low). The largest cleft holds more Upd resulting in higher concentrations and presumably biasing high STAT activation along that axis. The inset shows end-on activation patterns; STAT activated cells with suprathreshold level of Upd are marked with green stars.

qualitatively captures bistability and has the potential to be quantitatively more accurate. One key finding from this work was that sensitivity analysis of the bistable range suggested that changes in Apt translation and degradation rates had the greatest effect. The benefit of explicitly representing specific mechanisms, such as microRNAs, with some level of detail comes in the ability to cross check model results with experiments that genetically modify these mechanisms. Details of several reactants such as microRNAs and other regulators that have more recently been shown to affect border cell fate determination (for example [24,25,33–37]) can next be incorporated into this more mechanistic model, which could further clarify how bistability is molecularly controlled. This may also reveal where there are gaps in our genetic understanding of the process.

2.2. Born to run: Modeling confirms that tissue geometry can affect the spatial distribution of cytokine and activation pattern of border cells

STAT activation occurs in a graded fashion in anterior follicle cells, implying that cells more distant from the polar cells receive less of the pathway activator Upd compared to those close by (Fig. 2A-B). Only those cells with the highest levels of STAT activation become motile border cells; cells with intermediate signaling shut off the pathway due to bistability of the circuit described above. Given this significant role of the spatial distribution of Upd, we postulated that nurse cell geometry adjacent to the polar cells would impact the secreted activator.

Manning et al. [38] viewed the egg chamber "end on" allowing for the first time an anterior view of STAT activation patterns. A radially symmetric activation pattern would be expected from isotropic diffusion of cytokines from the polar cells. Remarkably, this was not the predominant pattern. Instead, three other patterns also emerged: a gap in the radially symmetric pattern, two gaps (eg, Fig. 2C and 2C'), or all cells specified to one side of the polar cells. A mathematical model for Upd diffusion and uptake along boundaries within a three-dimensional domain (Ω) mimicking nurse cell shapes allowed us to test the hypothesis that the tissue geometry is definitive in structuring activation patterns like those seen *in vivo*. We used the following equation and boundary conditions (Eq 1–Eq 4):

Box 1

.

Starz-Gaiano et al., 2008

Jak/STAT: $\frac{\partial J}{\partial t} = \frac{p_j U}{1 + q_j P^2 + 0.1J^2 + 33A^2/(1 + k_j S)} - r_j J$

Upd: $\frac{\partial U}{\partial t} = p_u P - r_u U + D_u \frac{\partial^2 U}{\partial x^2}$

Apt: $\frac{\partial A}{\partial t} = \frac{p_a J}{1 + 4A^2 + S} - r_a A + b_a$

Slbo: $\frac{\partial S}{\partial t} = \frac{p_S J^2}{1 + q_s A^2} - r_s S$

Yoon et al., 2011

Jak/STAT: $\frac{\partial J}{\partial t} = \frac{p_j U}{1 + q_j P^2 + a_j R/(1 + k_j S^2)} - r_j J$

Upd: $\frac{\partial U}{\partial t} = p_u P - r_u U + D_u \frac{\partial^2 U}{\partial x^2}$

Apt: $\frac{\partial A}{\partial t} = \frac{p_a J}{1 + q_a S} - r_a A + b_a$

Slbo: $\frac{\partial S}{\partial t} = \frac{p_S J^2}{1 + q_s A} - r_s S$

miR-279: $\frac{\partial R}{\partial t} = \frac{p_r A}{1 + q_r K^2} - r_r R$

Ken: $\frac{\partial K}{\partial t} = p_k J - r_k K$

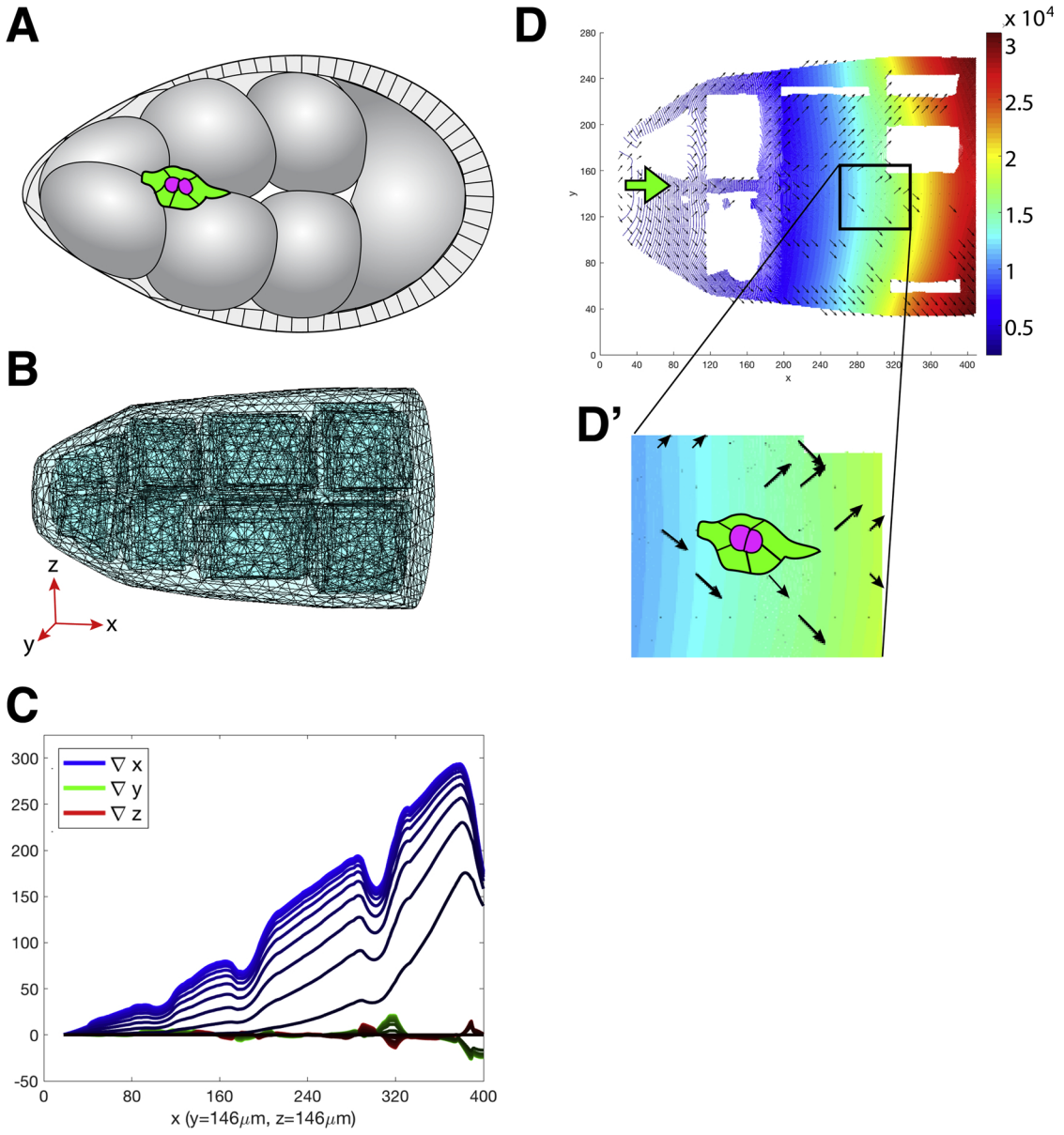

Fig. 3. Guidance signals may be impacted by tissue structure. A) Stage 9 egg chamber illustrates that germline cells (gray) fill much but not all of the available space created by the follicular epithelium boundary. B) Discretization of the 3D geometry created by nurse cell boundaries. C) When the distribution of chemoattractant is simulated in this domain, sharp drops in gradients are evident at the nurse cell junctions. D) One plane showing chemoattractant distribution and gradient vector fields from simulation. D') Inset from D showing that a border cell cluster may experience different vector directions on different sides as it moves along the central egg chamber axis. Panels B–D adapted from [43].

$$\frac{\partial u}{\partial t} = \nabla \cdot (D\nabla u) = D\left(\frac{\partial^2 u}{\partial x^2} + \frac{\partial^2 u}{\partial y^2} + \frac{\partial^2 u}{\partial z^2}\right), \ (x, y, z) \in \Omega \quad (1)$$

$$-D\frac{\partial u}{\partial z}\Big|_{\text{apical side of polar cells}} = \sigma \quad (2)$$

$$-D\frac{\partial u}{\partial z}\Big|_{\text{apical side of follicle cells}} = -ku \quad (3)$$

$$-D\nabla u \cdot \boldsymbol{n}|_{\text{all other boundaries}} = 0 \quad (4)$$

The first equation is simple diffusion in the extracellular space. The second equation describes Upd secretion with fixed rate σ, while the third and fourth equations represent uptake with rate k of Upd by the follicle cells and no-flux conditions at the other boundaries, such as nurse cells, respectively.

While nurse cells are mostly space-filling, their large size and bounded interior viscosity precludes them from filling all of the space underlying the follicular epithelium. Thus, a narrow crevasse or cleft can be observed where two nurse cells meet and abut the follicle cell layer (Fig. 2). While the width of the cleft is usually narrow relative to a cell diameter, it is large relative to a diffusible protein. Egg chambers commonly have three nurse cells that converge close to the polar cells, so domains were modeled with Y-shaped clefts (Fig. 2C-D). These clefts could reduce or expand activation patterns depending on their size and the time of simulation. Varying the width and depth of one arm of the cleft, Manning et al. [38] robustly reproduced the four patterns of cell

activations identified in experiments (an example is shown in Fig. 2D'). This confirmed the hypothesis that tissue geometry is sufficient to explain seemingly irregular, asymmetric STAT activation patterns and the corresponding specification of border cells. We speculate that this mechanism is advantageous in that it pre-aligns motile cells with their future path between nurse cells. As this model relied on the kinetics of better-known morphogens, current work aims to observe and measure Upd kinetics in a more direct manner, which could inform and improve the model.

2.3. Navigating the terrain: Geometry of the egg chamber influences cell fate and migration dynamics

How does the egg chamber microenvironment impact clustered cell migration? Tissue geometry matters in the distribution of a chemical signal secreted from a restricted domain, as discussed for cytokines in Section 2.2, and this too could impact the ways in which the border cell cluster migrates and how individual cells behave. Several chemoattractants are necessary and sufficient to guide the border cells [39–42], and are predominantly generated in the oocyte, presumably creating a gradient that decreases in intensity towards the anterior side, where the border cells originate. In most current models, the gradient of chemoattractant can direct the migratory forces, with cells moving toward higher concentrations of signal, typically along a central linear path through the egg chamber. However, the chemoattractant is not likely dispersed only along the central axis of the egg chamber, and the cluster response is not only one dimensional. For example, relocating the source of chemoattractant to a lateral position genetically causes the cluster to mis-migrate to that new location outside of the central axis [41,42]. In Mekus et al. [43], we incorporated explicit egg chamber geometry using finite element discretization and meshing in Matlab to model this structural effect on chemoattractant distribution and its subsequent impact on clustered cell migration.

We model chemoattractant movement as a reaction-diffusion equation with degradation throughout the domain (Eq 5) and secretion on the boundary (Eq 6), typically at the oocyte, and with potential uptake at the nurse cells (Eq 7). All other boundaries are no-flux (Eq 8).

$$\frac{\partial u}{\partial t} = D\left(\frac{\partial^2 u}{\partial x^2} + \frac{\partial^2 u}{\partial y^2} + \frac{\partial^2 u}{\partial z^2}\right) - ku \tag{5}$$

$$-D\frac{\partial u}{\partial n}\Big|_{\text{boundary source of chemoattractant}} = \sigma \tag{6}$$

$$-D\frac{\partial u}{\partial n}\Big|_{\text{boundary of nurse cells}} = -\phi u \tag{7}$$

$$-D\frac{\partial u}{\partial n}\Big|_{\text{all other boundaries}} = 0 \tag{8}$$

While overall an increasing amount of chemoattractant can be seen across the central axis of the egg chamber in this realistic geometry, fluctuations in the levels are evident (Fig. 3). Specifically, distribution of the chemoattractants laterally, especially at junctions where four nurse cells abut, results in dramatic dips in the gradients in all three dimensions (Fig. 3C and D). Because of this, within the narrow region spanned by the border cell cluster, cells on different sides might experience different directional gradients (Fig. 3D'). Currently the modeled extracellular space is greater than is physiological due to computational restrictions. This will affect the gradient between nurse cells with an increase in chemoattractant level, though the qualitative structure of the gradient may be similar. If the border cells sample the environment, for example through protrusions, to evaluate graded levels of chemoattractant, this difference in directional signals could contribute to the rotary behavior that is observed. Finding and incorporating a reasonable movement mechanism, such as nonlinear cell-cell repulsion with nonlinear membrane stiffness interactions, to the full dynamic simulation of the chemoattractant distribution such as from Mekus et al. [43] will be useful to hypothesize how the cells interpret these cues. Experimental characterization of where active chemoattractants are concentrated may help clarify how this model reflects the *in vivo* situation, and point to strategies to improve it further.

3. Collective migration

Soon after the motile cells are specified, the chemoattractant gradient has probably already developed and the border cell cluster begins its journey to the oocyte, which takes several hours [1,5,6,12]. The outer border cells respond to chemoattractant cues by remodeling their cytoskeleton, extending protrusions, altering adhesive contacts and shifting their position using the nurse cells as a substrate. The polar cells remain central to the cluster, where they promote continuous STAT signaling, but they do not exhibit motility. This mixed-cell-type cluster presents an interesting case for investigating how groups of cells move coordinately. In light of recent findings suggesting that some metastatic carcinomas migrate as a cohort, these coordinated cell-cell interactions are of particular interest [1,44–46].

3.1. May the force be with you: Force-balance representations in cell interactions allow for a quantitative look at clustered cell migration

A variety of mathematical models have been created to capture the essential dynamics of single cell migration, which is most often characterized by reiterated cycles of forward protrusion, adhesion, and detachment/retraction from the back (eg, Fig. 4A–D, reviewed in [47–50]. While there are multiple models for sheet-based movements with a front of migratory cells (for example [51–53]), fewer models have attempted to simulate coordinated movements of multiple, distinct cell types translocating as a small group (although some notable work has modeled the movements of Zebrafish lateral line clusters, eg [4,54]). Migratory cells must change shape and cyclically adhere and detach to a substrate to translocate. Clusters of cells may then have to adhere consistently to some local cells but break and re-form their physical connections to others. Coordinated migration is further complicated in that motile cells have to balance force generation between themselves and the substrate they move through, as well as with other moving cells to maintain a net positive forward migration. In the case of the border cell cluster, because the polar cells are non-motile, there may be an additional constraint on specifying a large-enough number of migratory cells to "carry" the polar cells and maintain them in the center of the group, without becoming burdensomely large. How do clusters of motile and non-motile cells cooperate to migrate effectively across the egg chamber? Modeling has led to some insights into these mechanisms.

Our laboratories have developed a force-balance based model for characterizing border cell migration where we effectively discretize our egg chamber into small units called Individual Math Cells (IMC, Fig. 4E). Single IMCs can represent individual follicle cells, while large sets of IMCs represent the nurse cells [55]. This choice provides the simplicity of the lattice-free agent-based model, which has been used for other collective cell migrations such as Zebrafish lateral line and neural crest [54,56], while maintaining the ability to represent force transmission between cells of vastly different sizes in a reasonable way. Furthermore, using interaction boundaries around domains of interaction with a defined capture radius but not hard boundaries allows flexibility when considering extracellular space, unlike with space filling frameworks such as cellular Potts models [57,58] or tessellations,

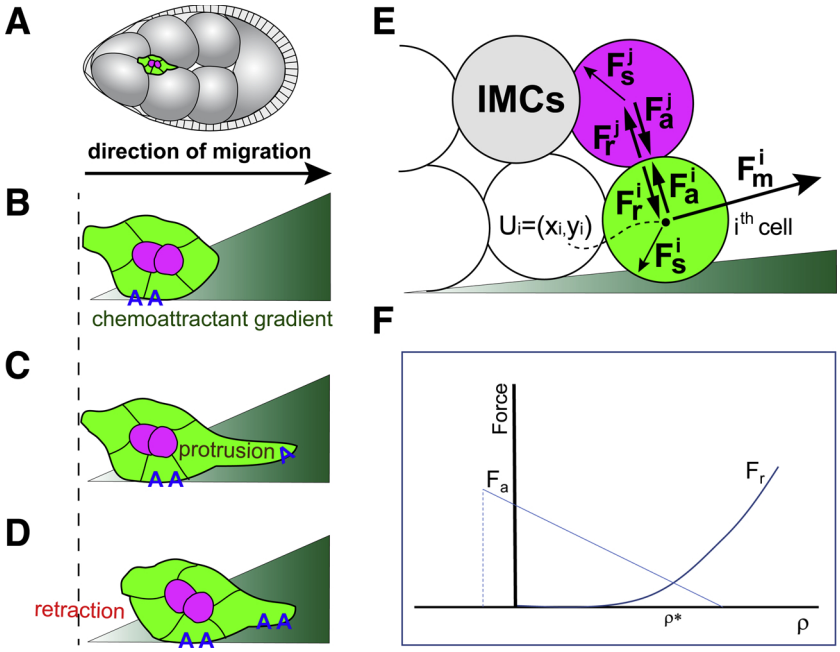

Fig. 4. Migratory forces. A) Stage 9 egg chamber with a migrating border cell cluster. Border cells, green, polar cells, magenta. B–D) The general cycle of cell migration along an increasing chemoattractant gradient. Adhesion molecules are represented by "As". B) Cells detect chemoattractant by cell surface receptors. C) The leading cell extends a long, actin-rich protrusion in the direction to move, and adheres at this location. D) Trailing cells are pulled by adhesion to the leading cell and myosin contraction at the back. Sites of adhesion must be remodeled: removed at the back and added at the front. E) Individual math cells (IMC) are identified by location ($U_i = (x_i, y_i)$) and can be used to represent the border cells (green), polar cells (magenta), other epithelial cells (white), or germline cells (gray), and modeled with the forces of adhesion (F_a), repulsion (F_r), stochasticity (F_s), or migration (F_m). F) Force balance overlap ρ between adhesion and repulsion.

such as Voronoi tessellations [59]. Thus, within the defined three-dimensional domain of the egg chamber, $\mathbb{R}^3$, U_i is the position in the i^{th} IMC, which can either represent a border cell, polar cell, or subcomponent of a larger nurse cell. The subscript $k \in \{a, r, s, m\}$ for force F_k indicates which of the adhesive (a), repulsive (r), stochastic (s), or migratory (m) forces are involved, and μ is the viscosity coefficient. Adhesive forces are needed to keep the cluster together and to provide traction, which typically in border cell migration is attributed to the homophilic adhesion molecule E-cadherin; repulsive forces are invoked due to the limits on compressibility as the cells squeeze together; migratory forces orient along the chemoattractant gradient. Thus, the equation for the i^{th} IMC is:

$$\mu \frac{dU_i}{dt} = \sum_j F_k^{ij}$$

for all other j cells.

Various mathematical forms, say piecewise linear, polynomial, or exponential, can represent different forces. For repulsive and adhesive forces, a balance of opposing forces (or an effective combined force) tends to have a larger radius of capture (negative overlap, ρ) for strong adherence and minimal repulsion countered by high repulsive force that overwhelms adhesion when cells come too close together. This yields, in the absence of other forces, a balance overlap, ρ* (Fig. 4F).

Including a stochastic force provides a way of introducing random sampling of the space by protrusions more than, say thermal fluctuations. This is addressed in a polarity term in other models (see below and [60]). A chemical signal that drives the migration in the proper direction induces the force to move. When polar cells are modeled, their migratory force can be set to zero as they are unable to migrate independently. Simple models can generate force by allowing individual border cells to interpret a gradient of chemoattractant by responding with force along the increasing gradient [55], even when the signal is distributed in more complex patterns than a linear or exponential gradient in one direction (eg [43], and see Section 2.3). Recently force generation has been modeled taking into account the spatial extent (size) of the cluster [61]:

$$F_x = \int_0^{\pi} 2\pi S(x_0 + R\cos\theta) R^2 \cos\theta \sin\theta d\theta$$

where $S(x)$ is the saturating receptor response (force per volume) to the chemoattractant concentration at x. Here all of the concentration is added up at the surface of a cluster of radius R and the force, $F_x(x_0)$, is dependent on x_0.

In another model, additional force-like terms have been added to the position equation to capture persistence in a particular direction using polarization. Migrating cells in a petri dish will often continue to move in one direction in the absence of new signals in the environment. When such motile cells collide, though, they often reverse direction, referred to as contact inhibition of locomotion (CIL) (reviewed in [62]). How this inhibition affects cells in motile clusters is less clear since these cells are in constant contact. Camley et al. [60] added an additional polarity term, p^i, to the position equation and the polarity satisfies the equation:

$$\frac{dp^i}{dt} = \frac{1}{\tau} p^i + \xi(t) + \beta^i q^i$$

where τ is a time constant for polarization persistence, ξ is a Gaussian random perturbation, and q^i is a vector biasing the polarization away from neighboring cells with a weight factor β^i. This weight factor is interpreted as a cell's susceptibility to CIL and may depend on chemoattractant, $\beta^i(S(x))$, but does not require each individual cell of the cluster to interpret a gradient; instead directional movement emerges from the collection.

3.2. Size versus speed: How models inform velocity and migratory cohort size

Collective cell migration can occur for very small or quite large groups of cells, depending on context. In the typical egg chamber, six border cells surround two non-motile polar cells throughout the migration event. Presumably, this ratio is optimized to provide enough motile cells to exert the force needed to move the non-motile cells while being small enough to fit through the constrained spaces within the egg

chamber. The Camley et al. [60] model admits migration for clusters of cells as small as two, which can be made to occur *in vivo*, but without polar cells. When the polar cells are modeled as non-motile, such as by Stonko et al. [55], at least 6 motile cells are necessary to enable migration to occur at the relevant timescale. In several models [55,60,61], increasing the number of motile cells can increase the overall velocity - up to a limit (see below), which is also consistent with experiments that conversely reduce border cell number and decrease successful migration. Proper control of velocity is important since delays in migration timing can result in a failure of the cells to contribute to the developing egg, rendering it inviable.

Interestingly, the velocity of border cell cluster migration decreases on average as the border cell cluster gets closer to the oocyte [8–10,63,64]. The velocity of the cluster center or individual border cells within the cluster can be calculated from a dynamic migration model [43,55], and theoretical derivations of mean velocity in terms of model parameters can assist in identifying certain system characteristics. Stonko et al. [55] found variability in speed but not a consistent decrease. The force generation model in Cai et al. [61] based on the surface integral of chemoattractant allowed them to approximate the mean cluster velocity by

$$\langle V_c \rangle = \frac{F_x}{\lambda}$$

where λ is the damping viscosity coefficient, which they take in two parts as adhesive viscosity and viscosity due to nurse cells, λ_{visc}. Camley et al. [60] estimates mean velocity of the cluster of cells at r^i as it depends upon the sum of the CIL from the neighboring cells, r^j, and the total number of cells, N,

$$\langle V_c \rangle = \frac{\bar{\beta}\tau}{N} \sum_i S(r^i) \sum_{j \sim i} \frac{(r^i - r^j)}{|r^i - r^j|}$$

Through either simulation or theory, the models yielded a common result: that velocity tended to increase when cluster size increased, leveling off for large cluster size. However, results of experiments in which cluster size had been manipulated showed a steep drop off in migration speed above a certain cluster size (about 26 μm). Cai et al. [61] proposed that the lateral confinement of the egg chamber due to a surrounding layer of extracellular matrix (ECM) causes the increase in viscosity coefficient and the precipitous drop in velocity. They supposed that $\lambda_{visc} = 6\pi\mu R/(1 - R/26\mu m)$ was increased dramatically in proportion to cluster radius beyond the critical cluster size, and were able to reproduce the dramatic fall off in the speed profile.

3.3. Autocracy versus democracy: Guiding directional movement for a group of independent cells

How do clusters of border cells function together to migrate effectively across the egg chamber? The mechanism of how any cell interprets a gradient remains a compelling open research area, although local activation/global inhibition models accurately capture behaviors for individual cells (eg, see [65]). The chemoattractants that guide the border cells include several epidermal growth factor (EGF) receptor ligands, and a protein ligand family that shares homology with both platelet-derived growth factor (PDGF) and vascular endothelial growth factor (VEGF) [39–42]. These signals are predominantly generated in the oocyte, presumably creating a gradient across the egg chamber. More work is needed to determine the quantities and relevant distribution of these signals *in vivo*. The chemoattractants bind to receptor tyrosine kinases at the border cell surface, which triggers a series of coordinated cytoskeletal changes (eg, [6,8,10,66–72] and see below). An interesting aspect of the Camley et al. (2016) [60] model is that as long as there are two cells and CIL, the gradient is not needed, only the presence of chemoattractant. This is reminiscent of other models in which uniform chemoattractant can lead to directional migration as long as cells start at one side of a domain and use up the signal as they migrate [73–75]. Other studies suggest a tension gradient acting through E-cadherin may also provide guidance information [76] or that high tension in the nurse cells via the actinomyosin network must be counter-balanced by increased tension in border cells, which promotes efficient movement [77].

Many well-studied collective migrations feature specific cells that act as leaders [7,78]. One curious behavior observed from live imaging of border cell migration is that the cluster appears to rotate along a central polar cell axis, with different border cells jockeying for the front position [8–10,63]. Experimentalists postulated a molecular mechanism for this outcome: chemoattractant receptors at the front of the cluster become saturated for signal, resulting in next-neighbors with still unoccupied receptors to experience increased signaling and move ahead [8,63]. Stonko et al. [55] suggest a different model that stems from the biophysics: The gaps at intersections between nurse cells reduce adhesion in those locations, thus slowing down the border cells and forcing them to rotate towards the next available attachment point. Simulations showed border cells switching positions. These models are not mutually exclusive, and it is likely that both - and the mechanism described in **2.3**, which results in variations in chemoattractant gradient direction on different sides of the cluster - contribute to the dynamic behaviors observed. There may also be additional or alternative explanations. Rotating cell behaviors have been attributed to additional mechanisms found in other tissues, such as coherent angular motion (CAMo) in human mammary tissue [79], emergent rotation from boundedness by ECM [80], and rotation observed in B and T lymphocytes modeled using polarization, adhesion-repulsion and chemoattractant forces, and long range spring-like force, which reproduces related experimental observations [81,82]. Thus, these other mechanisms are worth further investigation in ovarian cells.

During migration, the border cells appear to communicate to each other about who is the current leader in the cluster, as revealed from elegant experiments in which one cell was induced to move at a time [72]. These experiments took advantage of a known cytoskeletal regulator, the small monomeric GTPase Rac. Cytosolic Rac, in its GTP-bound, activated form, promotes local formation of actin-rich protrusive structures such as filopodia, and is required for diverse types of cell migrations [83,84]. When Wang et al. [72] forced one cell to move at a time through increased, localized Rac photo-activation, surprisingly, other cells in the group were repressed from adopting motile shapes and actin-based protrusions. Although there are some molecular clues to how this could be regulated, potentially through mechanical tension, gap junctions, or other signaling molecules (eg, [72,85,86], it is not known what directs the communication, or how it influences known signaling pathways in these cells.

A difficulty with detailed kinetic models is often the lack of experimental details to determine reaction parameters. Then determining the general positive or negative functional forms is a reasonable outcome of modeling. However, sometimes even that detail of interaction is unclear. In that case, even simply understanding the directions of the biochemical signaling network is a challenge. To study how different known signals relate in this context, that is to determine the topology of border cell migration signaling, Yue et al. [87] used experimental information to determine possible interactions between four key components of the process: chemoattractant, cell activation through Rac, protrusion, and a global signal in a cell's ability to move (Fig. 5). They then examined the relationships between these components and found that six connections between elements are necessary for a minimal model to capture the outcomes from sets of experiments inhibiting or relocating cell activation through Rac and knocking down chemoattractant receptors [10,72]. Based on known interactions, all topologies had three connections preset: a chemoattractant (Signal, S) activates Rac (R), Rac activates protrusions (P), and protrusions are further self-activating. Then, different topology models could be designed and tested to determine potential roles for the global cell-cell

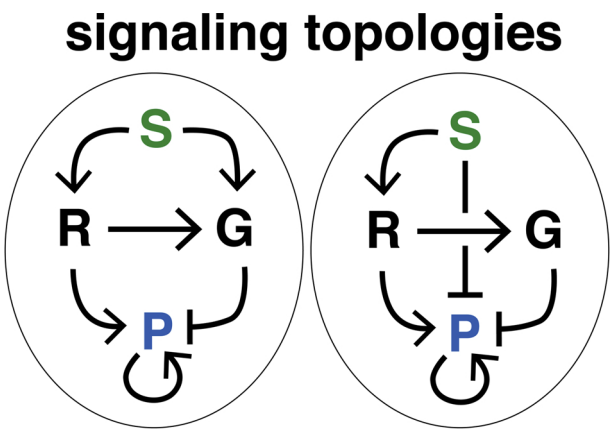

Fig. 5. Two possible molecular signaling topologies predicted by Yue et al. [87] to explain border cell behaviors*in vivo*. Activating chemoattractant (Signal, S) activates Rac (R), which activates actin-rich protrusions (P), and protrusions are further self-activating. A global cell-cell communication signal (G) is also required to capture known protrusive behaviors of the cells. Yue et al. narrowed down thousands of topology to six more likely cases, including these.

communication signal (G). After simulations and sensitivity tests, six topologies (of the six connection minimal networks, of thousands of possibilities) satisfied the given experiments and more detailed kinetic model parameters were determined for each case. For example, one topology (Fig. 5 left) has the additional connections of chemoattractant and Rac activating the global signal and the global signal inhibiting protrusions, while in another topology (Fig. 5 right), rather than chemoattractant activating the global signal, the chemoattractant inhibits protrusions directly. With the six different yet potentially valid topologies, further experimental information is required to refine the appropriate network, which the authors suggest could come from velocity estimates.

The velocity profiles for each topology over an exponential gradient captures the increase followed by slowing down, which is also described in the Cai et al. [61] model and seen in the Mekus et al. [43] simulations. However, each of the six velocity profiles varies, and some show quite dramatic changes over time. It is not clear how much variation in a velocity profile might come from a different topology or a different valid parameter set within a given topology, which makes deciding on the most appropriate topology still a challenge. Obviously more complex topologies are also possible. Interestingly, Prasad and Montell [10] blocked guidance receptor signaling in all motile cells by expression of a dominant negative receptor and found additional protrusions, which seems likely to confound a global signal and may suggest that the topology without direct inhibition from S to P is less likely (Fig. 5, left). Yue et al. [87] propose that blocking gap junctions in border cells might provide a clue to how the communication signal works, although knock down of Innexin2 has a partial phenotype [86], suggesting other players need to be tested. A caveat to the topologies is that the existence of protrusions *in vivo* does not directly translate into forward movement; instead, multiple protrusions may extend in different directions, and movement may follow only the largest or most persistent one. However the selected topologies do indicate that the unspecified global communication signal is critical in positive cluster progression, and the new proposed connections that these models suggest to the known network may help in identification of this signal.

4. Discussion and future directions

The specification and migration of border cells as a cluster around the initiating polar cells within the *Drosophila melanogaster* egg chamber is a model system for understanding cell migration in development, immune response, and metastasis. In this brief review we have focused on several aspects of the border cells that are amenable to mathematical modeling and analysis including intracellular signaling, extracellular geometry modulating signaling, and forces affecting clustered cell migration. The intracellular signaling switch that determines the cell fate due to cross repression between two transcription factors, Apt and Slbo, has been qualitatively described mathematically [29–31] as well as quantitatively modeled, though only with incomplete kinetic parameters ([32] and our unpublished data). Initiation of this intracellular decision occurs through extracellular cytokine diffusion and depends remarkably on the egg chamber geometry, specifically on the narrow spaces between germline and follicle cells [38]. Extracellular geometry continues to impact the formed cluster by chemoattractant percolating around germline cells to deliver the guidance cues for migration and by the germline cells providing both adhesive support and resistance to the migrating cluster. Force balance equations in agent-based models dominate clustered cell modeling with some exceptions such as using continuum approximations of discrete cellular conglomerations found in phase field models [88]. Some of these agent-based models consider the impact of the extracellular geometry [43,55,61]. Significant analysis has been applied to capturing the velocity and cluster characteristics [60,61,87], however, simplifying assumptions often eliminate the realistic geometry.

Future advances in experimental techniques and feedback into the models are needed to refine our understanding. For example, several theories will be advanced by the ability to measure chemoattractant in the tight extracellular spaces *in vivo*, and allow for key comparisons with model predictions. These model predictions will also act to drive experimental innovation to test their accuracy. More details in the intracellular signaling pathways controlling cell fate and migration processes will allow for further refinement of mathematical models leading to specific, experimentally-testable predictions. Measuring the signaling activity of biologically active molecules like Rac while experimentally modulating other aspects of the system will allow for much clearer information on cell-to-cell or global communication cues. It is likely that some of the subcellular mechanics described in other articles in this Special Issue may be applicable to the border cell clusters and yield multiscale models that can link subcellular defects (or enhancements) to global behavior. Additionally, continued genetic analysis is likely to reveal new essential regulators. By combining the sophisticated genetic manipulations and well-characterized developmental biology of Drosophila with mathematical tools and analysis, the border cell system will likely provide increasingly clear explanations of how groups of cells move through space and time.

Acknowledgements

We acknowledge support through National Science Foundation grantIOS-1656550to MSG. We thank M. Bhattacharya, A. George, S. Trivedi, and K. Hoffman for helpful comments on the manuscript.

References

[1] C.H. Stuelten, C.A. Parent, D.J. Montell, Cell motility in cancer invasion and metastasis: insights from simple model organisms, Nat. Rev. Cancer 18 (5) (2018) 296–312, https://doi.org/10.1038/nrc.2018.15.
[2] M. Cetera, S. Horne-Badovinac, Round and round gets you somewhere: collective cell migration and planar polarity in elongating Drosophila egg chambers, Curr. Opin. Genet. Dev. 32 (2015) 10–15, https://doi.org/10.1016/j.gde.2015.01.003.
[3] J.C. Duhart, T.T. Parsons, L.A. Raftery, The repertoire of epithelial morphogenesis on display: progressive elaboration of Drosophila egg structure, Mech. Dev. 148 (2017) 18–39, https://doi.org/10.1016/j.mod.2017.04.002.
[4] A. Aman, T. Piotrowski, Cell migration during morphogenesis, Dev. Biol. (Basel) 341 (1) (2009) 20–33 S0012-1606(09)01360-8 [pii] /j.ydbio.2009.11.014.
[5] A. Saadin, M. Starz-Gaiano, Circuitous genetic regulation governs a straightforward cell migration, Trends Genet. 32 (10) (2016) 660–673, https://doi.org/10.1016/j.tig.2016.08.001.
[6] D.J. Montell, W.H. Yoon, M. Starz-Gaiano, Group choreography: mechanisms orchestrating the collective movement of border cells, Nat. Rev. Mol. Cell Biol. 13

(10) (2012) 631–645, https://doi.org/10.1038/nrm3433.
[7] P. Rorth, Fellow travellers: emergent properties of collective cell migration, EMBO Rep. 13 (11) (2012) 984–991, https://doi.org/10.1038/embor.2012.149.
[8] A. Bianco, M. Poukkula, A. Cliffe, J. Mathieu, C.M. Luque, T.A. Fulga, P. Rorth, Two distinct modes of guidance signalling during collective migration of border cells, Nature 448 (7151) (2007) 362–365.
[9] M. Prasad, A.C. Jang, M. Starz-Gaiano, M. Melani, D.J. Montell, A protocol for culturing Drosophila melanogaster stage 9 egg chambers for live imaging, Nat. Protoc. 2 (10) (2007) 2467–2473.
[10] M. Prasad, D.J. Montell, Cellular and molecular mechanisms of border cell migration analyzed using time-lapse live-cell imaging, Dev. Cell 12 (6) (2007) 997–1005.
[11] H. Tekotte, D. Tollervey, I. Davis, Imaging the migrating border cell cluster in living Drosophila egg chambers, Dev. Dyn. 236 (10) (2007) 2818–2824, https://doi.org/10.1002/dvdy.21305.
[12] P. Rorth, Initiating and guiding migration: lessons from border cells, Trends Cell Biol. 12 (7) (2002) 325–331 S0962892402023115 [pii].
[13] R.C. King, Ovarian Development in Drosophila melanogaster, Academic Press, New York, 1970.
[14] S. Beccari, L. Teixeira, P. Rorth, The JAK/STAT pathway is required for border cell migration during Drosophila oogenesis, Mech. Dev. 111 (1–2) (2002) 115–123.
[15] C. Ghiglione, O. Devergne, E. Georgenthum, F. Carballes, C. Medioni, D. Cerezo, S. Noselli, The Drosophila cytokine receptor Domeless controls border cell migration and epithelial polarization during oogenesis, Development 129 (23) (2002) 5437–5447.
[16] D.L. Silver, D.J. Montell, Paracrine signaling through the JAK/STAT pathway activates invasive behavior of ovarian epithelial cells in Drosophila, Cell 107 (7) (2001) 831–841.
[17] D.L. Silver, E.R. Geisbrecht, D.J. Montell, Requirement for JAK/STAT signaling throughout border cell migration in Drosophila, Development 132 (15) (2005) 3483–3492.
[18] R. Xi, J.R. McGregor, D.A. Harrison, A gradient of JAK pathway activity patterns the anterior-posterior axis of the follicular epithelium, Dev. Cell 4 (2) (2003) 167–177.
[19] S. Trivedi, M. Starz-Gaiano, Drosophila Jak/STAT signaling: regulation and relevance in human Cancer and metastasis, Int. J. Mol. Sci. 19 (12) (2018), https://doi.org/10.3390/ijms19124056.
[20] N.I. Arbouzova, M.P. Zeidler, JAK/STAT signalling in Drosophila: insights into conserved regulatory and cellular functions, Development 133 (14) (2006) 2605–2616.
[21] S.C. Herrera, E.A. Bach, JAK/STAT signaling in stem cells and regeneration: from Drosophila to vertebrates, Development 146 (2) (2019), https://doi.org/10.1242/dev.167643.
[22] Q. Chen, M. Giedt, L. Tang, D.A. Harrison, Tools and methods for studying the Drosophila JAK/STAT pathway, Methods 68 (1) (2014) 160–172, https://doi.org/10.1016/j.ymeth.2014.03.023.
[23] D.A. Harrison, P.E. McCoon, R. Binari, M. Gilman, N. Perrimon, Drosophila unpaired encodes a secreted protein that activates the JAK signaling pathway, Genes Dev. 12 (20) (1998) 3252–3263.
[24] V. Van de Bor, G. Zimniak, D. Cerezo, S. Schaub, S. Noselli, Asymmetric localisation of cytokine mRNA is essential for JAK/STAT activation during cell invasiveness, Development 138 (7) (2011) 1383–1393 dev.056184 [pii] /dev.056184.
[25] A. Saadin, M. Starz-Gaiano, Cytokine exocytosis and JAK/STAT activation in the Drosophila ovary requires the vesicle trafficking regulator alpha-Snap, J. Cell. Sci. 131 (23) (2018), https://doi.org/10.1242/jcs.217638.
[26] L. Wang, T.R. Sexton, C. Venard, M. Giedt, Q. Guo, Q. Chen, D.A. Harrison, Pleiotropy of the Drosophila JAK pathway cytokine Unpaired 3 in development and aging, Dev. Biol. (Basel) 395 (2) (2014) 218–231, https://doi.org/10.1016/j.ydbio.2014.09.015.
[27] J.R. McGregor, R. Xi, D.A. Harrison, JAK signaling is somatically required for follicle cell differentiation in Drosophila, Development 129 (3) (2002) 705–717.
[28] D.J. Montell, P. Rorth, A.C. Spradling, slow border cells, a locus required for a developmentally regulated cell migration during oogenesis, encodes Drosophila C/EBP, Cell 71 (1) (1992) 51–62 0092-8674(92)90265-E [pii].
[29] M. Starz-Gaiano, M. Melani, X. Wang, H. Meinhardt, D.J. Montell, Feedback inhibition of Jak/STAT signaling by apontic is required to limit an invasive cell population, Dev. Cell 14 (5) (2008) 726–738 S1534-5807(08)00113-5 [pii] /j.devcel.2008.03.005.
[30] W.H. Yoon, H. Meinhardt, D. Montell, miRNA-mediated feedback inhibition of JAK/STAT morphogen signalling establishes a cell fate threshold, Nat Cell Biol in press/online (2011).
[31] M. Starz-Gaiano, M. Melani, H. Meinhardt, D. Montell, Interpretation of the UPD/JAK/STAT morphogen gradient in Drosophila follicle cells, Cell Cycle 8 (18) (2009) 2917–2925.
[32] X. Ge, D.P. Stonko, Modeling a cellular response to a gradient mathematics and molecular biology inform a mechanistic understanding, Journal of Undergraduate Research UMBC Review 13 (2012) 90–112.
[33] A.J. Monahan, M. Starz-Gaiano, Socs36E attenuates STAT signaling to optimize motile cell specification in the Drosophila ovary, Dev. Biol. (Basel) 379 (2) (2013) 152–166, https://doi.org/10.1016/j.ydbio.2013.03.022.
[34] A.J. Monahan, M. Starz-Gaiano, Socs36E limits STAT signaling via Cullin2 and a SOCS-box independent mechanism in the Drosophila egg chamber, Mech Dev 138 Pt 3 (2015) 313–327, https://doi.org/10.1016/j.mod.2015.08.003.
[35] A. Saadin, M. Starz-Gaiano, Identification of novel regulators of the JAK/STAT signaling pathway that control border cell migration in the Drosophila ovary, G3 Bethesda (Bethesda) 6 (7) (2016) 1991–2002, https://doi.org/10.1534/g3.116.028100.
[36] Y. Hayashi, T.R. Sexton, K. Dejima, D.W. Perry, M. Takemura, S. Kobayashi, H. Nakato, D.A. Harrison, Glypicans regulate JAK/STAT signaling and distribution of the Unpaired morphogen, Development 139 (22) (2012) 4162–4171, https://doi.org/10.1242/dev.078055.
[37] G. Aranjuez, E. Kudlaty, M.S. Longworth, J.A. McDonald, On the role of PDZ domain-encoding genes in Drosophila border cell migration, G3 Bethesda (Bethesda) 2 (11) (2012) 1379–1391, https://doi.org/10.1534/g3.112.004093.
[38] L.A. Manning, A.M. Weideman, B.E. Peercy, M. Starz-Gaiano, Tissue landscape alters adjacent cell fates during Drosophila egg development, Nat. Commun. 6 (2015) 7356.10.1038/ncomms8356.
[39] P. Duchek, P. Rorth, Guidance of cell migration by EGF receptor signaling during Drosophila oogenesis, Science 291 (5501) (2001) 131-3.10.1126/science.291.5501.131 291/5501/131 [pii].
[40] P. Duchek, K. Somogyi, G. Jekely, S. Beccari, P. Rorth, Guidance of cell migration by the Drosophila PDGF/VEGF receptor, Cell 107 (1) (2001) 17–26.
[41] J.A. McDonald, E.M. Pinheiro, L. Kadlec, T. Schupbach, D.J. Montell, Multiple EGFR ligands participate in guiding migrating border cells, Dev. Biol. (Basel) (2006).
[42] J.A. McDonald, E.M. Pinheiro, D.J. Montell, PVF1, a PDGF/VEGF homolog, is sufficient to guide border cells and interacts genetically with Taiman, Development 130 (15) (2003) 3469–3478.
[43] Z. Mekus, J. Cooley, A. George, V. Sabo, M. Strzegowski, M. Starz-Gaiano, B.E. Peercy, Effects of cell packing on chemoattractant distribution within a tissue, AIMS Biophys. 5 (1) (2018) 1–21, https://doi.org/10.3934/biophy.2018.1.1.
[44] P. Friedl, D. Gilmour, Collective cell migration in morphogenesis, regeneration and cancer, Nat. Rev. Mol. Cell Biol. 10 (7) (2009) 445–457, https://doi.org/10.1038/nrm2720.
[45] P. Friedl, J. Locker, E. Sahai, J.E. Segall, Classifying collective cancer cell invasion, Nat. Cell Biol. 14 (8) (2012) 777–783, https://doi.org/10.1038/ncb2548.
[46] M. Lintz, A. Munoz, C.A. Reinhart-King, The mechanics of single cell and collective migration of tumor cells, J. Biomech. Eng. 139 (2) (2017), https://doi.org/10.1115/1.4035121.
[47] D.A. Lauffenburger, A.F. Horwitz, Cell migration: a physically integrated molecular process, Cell 84 (3) (1996) 359–369.
[48] M. Vicente-Manzanares, A.R. Horwitz, Cell migration: an overview, Methods Mol. Biol. 769 (2011) 1–24, https://doi.org/10.1007/978-1-61779-207-6_1.
[49] P. Devreotes, A.R. Horwitz, Signaling networks that regulate cell migration, Cold Spring Harb. Perspect. Biol. 7 (8) (2015) a005959.10.1101/cshperspect.a005959.
[50] A.J. Ridley, M.A. Schwartz, K. Burridge, R.A. Firtel, M.H. Ginsberg, G. Borisy, J.T. Parsons, A.R. Horwitz, Cell migration: integrating signals from front to back, Science 302 (5651) (2003) 1704–1709 10.1126/science.1092053/5651/1704 [pii].
[51] X.G. Peralta, Y. Toyama, M.S. Hutson, R. Montague, S. Venakides, D.P. Kiehart, G.S. Edwards, Upregulation of forces and morphogenic asymmetries in dorsal closure during Drosophila development, Biophys. J. 92 (7) (2007) 2583-96.S0006-3495(07)71062-7 [pii] 10.1529/biophysj.106.094110.
[52] R.E. Baker, A. Parker, M.J. Simpson, A free boundary model of epithelial dynamics, J. Theor. Biol. (2018), https://doi.org/10.1016/j.jtbi.2018.12.025.
[53] J.C. Arciero, Q. Mi, M.F. Branca, D.J. Hackam, D. Swigon, Continuum model of collective cell migration in wound healing and colony expansion, Biophys. J. 100 (3) (2011) 535–543, https://doi.org/10.1016/j.bpj.2010.11.083.
[54] H. Knutsdottir, C. Zmurchok, D. Bhaskar, E. Palsson, D. Dalle Nogare, A.B. Chitnis, L. Edelstein-Keshet, Polarization and migration in the zebrafish posterior lateral line system, PLoS Comput. Biol. 13 (4) (2017) e1005451.10.1371/journal.-pcbi.1005451.
[55] D.P. Stonko, L. Manning, M. Starz-Gaiano, B.E. Peercy, A mathematical model of collective cell migration in a three-dimensional, heterogeneous environment, PLoS One 10 (4) (2015) e0122799.10.1371/journal.pone.0122799.
[56] M. Yamao, H. Naoki, S. Ishii, Multi-cellular logistics of collective cell migration, PLoS One 6 (12) (2011) e27950.10.1371/journal.pone.0027950.
[57] J.A. Glazier, F. Graner, Simulation of the differential adhesion driven rearrangement of biological cells, Phys. Rev. E Stat. Phys. Plasmas Fluids Relat. Interdiscip. Topics 47 (3) (1993) 2128–2154, https://doi.org/10.1103/physreve.47.2128.
[58] N. Guisoni, K.I. Mazzitello, L. Diambra, Modeling active cell movement with the potts model, Front. Phys. 6 (2018) 61.10.3389/fphy.2018.00061.
[59] S. Kaliman, C. Jayachandran, F. Rehfeldt, A.S. Smith, Limits of applicability of the voronoi tessellation determined by centers of cell nuclei to epithelium morphology, Front. Physiol. 7 (2016) 551.10.3389/fphys.2016.00551.
[60] B.A. Camley, J. Zimmermann, H. Levine, W.J. Rappel, Emergent collective chemotaxis without single-cell gradient sensing, Phys. Rev. Lett. 116 (9) (2016) 098101, , https://doi.org/10.1103/PhysRevLett.116.098101.
[61] D. Cai, W. Dai, M. Prasad, J. Luo, N.S. Gov, D.J. Montell, Modeling and analysis of collective cell migration in an in vivo three-dimensional environment, Proc Natl Acad Sci U S A 113 (15) (2016) E2134-41.10.1073/pnas.1522656113.
[62] B. Stramer, R. Mayor, Mechanisms and in vivo functions of contact inhibition of locomotion, Nat. Rev. Mol. Cell Biol. 18 (1) (2017) 43–55, https://doi.org/10.1038/nrm.2016.118.
[63] M. Poukkula, A. Cliffe, R. Changede, P. Rorth, Cell behaviors regulated by guidance cues in collective migration of border cells, J. Cell Biol. 192 (3) (2011) 513–524 jcb.201010003 [pii] 10.1083/jcb.201010003.
[64] A. Cliffe, D.P. Doupe, H. Sung, I.K. Lim, K.H. Ong, L. Cheng, W. Yu, Quantitative 3D analysis of complex single border cell behaviors in coordinated collective cell migration, Nat. Commun. 8 (2017) 14905.10.1038/ncomms14905.
[65] C. Shi, C.H. Huang, P.N. Devreotes, P.A. Iglesias, Interaction of motility, directional sensing, and polarity modules recreates the behaviors of chemotaxing cells, PLoS Comput. Biol. 9 (7) (2013) e1003122.10.1371/journal.pcbi.1003122.
[66] C. Plutoni, S. Keil, C. Zeledon, L.E.A. Delsin, B. Decelle, P.P. Roux, S. Carreno, G. Emery, Misshapen coordinates protrusion restriction and actomyosin contractility during collective cell migration, Nat. Commun. 10 (1) (2019)

3940.10.1038/s41467-019-11963-7.
[67] J.A. McDonald, A. Khodyakova, G. Aranjuez, C. Dudley, D.J. Montell, PAR-1 kinase regulates epithelial detachment and directional protrusion of migrating border cells, Curr. Biol. 18 (21) (2008) 1659-67.S0960-9822(08)01271-2 [pii] 10.1016/j.cub.2008.09.041.
[68] Y.C. Chang, J.W. Wu, Y.C. Hsieh, T.H. Huang, Z.M. Liao, Y.S. Huang, J.A. Mondo, D. Montell, A.C. Jang, Rap1 negatively regulates the hippo pathway to polarize directional protrusions in collective cell migration, Cell Rep. 22 (8) (2018) 2160–2175, https://doi.org/10.1016/j.celrep.2018.01.080.
[69] K. Sawant, Y. Chen, N. Kotian, K.M. Preuss, J.A. McDonald, Rap1 GTPase promotes coordinated collective cell migration in vivo, Mol. Biol. Cell 29 (22) (2018) 2656–2673, https://doi.org/10.1091/mbc.E17-12-0752.
[70] E.P. Lucas, I. Khanal, P. Gaspar, G.C. Fletcher, C. Polesello, N. Tapon, B.J. Thompson, The Hippo pathway polarizes the actin cytoskeleton during collective migration of Drosophila border cells, J. Cell Biol. 201 (6) (2013) 875–885, https://doi.org/10.1083/jcb.201210073.
[71] X. Wang, L. He, Y.I. Wu, K.M. Hahn, D.J. Montell, Light-mediated activation reveals a key role for Rac in collective guidance of cell movement in vivo, Nat. Cell Biol. 12 (6) (2010) 591-7.ncb2061 [pii] 10.1038/ncb2061.
[72] A.J. Muinonen-Martin, O. Susanto, Q. Zhang, E. Smethurst, W.J. Faller, D.M. Veltman, G. Kalna, C. Lindsay, D.C. Bennett, O.J. Sansom, R. Herd, R. Jones, L.M. Machesky, M.J. Wakelam, D.A. Knecht, R.H. Insall, Melanoma cells break down LPA to establish local gradients that drive chemotactic dispersal, PLoS Biol. 12 (10) (2014) e1001966.10.1371/journal.pbio.1001966.
[73] O. Susanto, Y.W.H. Koh, N. Morrice, S. Tumanov, P.A. Thomason, M. Nielson, L. Tweedy, A.J. Muinonen-Martin, J.J. Kamphorst, G.M. Mackay, R.H. Insall, LPP3 mediates self-generation of chemotactic LPA gradients by melanoma cells, J. Cell. Sci. 130 (20) (2017) 3455–3466, https://doi.org/10.1242/jcs.207514.
[74] L. Tweedy, D.A. Knecht, G.M. Mackay, R.H. Insall, Self-generated chemoattractant gradients: attractant depletion extends the range and robustness of Chemotaxis, PLoS Biol. 14 (3) (2016) e1002404.10.1371/journal.pbio.1002404.
[75] D. Cai, S.C. Chen, M. Prasad, L. He, X. Wang, V. Choesmel-Cadamuro, J.K. Sawyer, G. Danuser, D.J. Montell, Mechanical feedback through E-cadherin promotes direction sensing during collective cell migration, Cell 157 (5) (2014) 1146-59.10.1016/j.cell.2014.03.045.
[76] G. Aranjuez, A. Burtscher, K. Sawant, P. Majumder, J.A. McDonald, Dynamic myosin activation promotes collective morphology and migration by locally balancing oppositional forces from surrounding tissue, Mol. Biol. Cell 27 (12) (2016) 1898–1910, https://doi.org/10.1091/mbc.E15-10-0744.
[77] R. Mayor, S. Etienne-Manneville, The front and rear of collective cell migration, Nat. Rev. Mol. Cell Biol. 17 (2) (2016) 97–109, https://doi.org/10.1038/nrm.2015.14.
[78] K. Tanner, H. Mori, R. Mroue, A. Bruni-Cardoso, M.J. Bissell, Coherent angular motion in the establishment of multicellular architecture of glandular tissues, Proc Natl Acad Sci U S A 109 (6) (2012) 1973-8.10.1073/pnas.1119578109.
[79] K. Doxzen, S.R. Vedula, M.C. Leong, H. Hirata, N.S. Gov, A.J. Kabla, B. Ladoux, C.T. Lim, Guidance of collective cell migration by substrate geometry, Integr. Biol. (Camb) 5 (8) (2013) 1026-35.10.1039/c3ib40054a.
[80] G. Malet-Engra, W. Yu, A. Oldani, J. Rey-Barroso, N.S. Gov, G. Scita, L. Dupre, Collective cell motility promotes chemotactic prowess and resistance to chemorepulsion, Curr. Biol. 25 (2) (2015) 242–250, https://doi.org/10.1016/j.cub.2014.11.030.
[81] K. Copenhagen, G. Malet-Engra, W. Yu, G. Scita, N. Gov, A. Gopinathan, Frustration-induced phases in migrating cell clusters, Sci. Adv. 4 (9) (2018) eaar8483.10.1126/sciadv.aar8483.
[82] C.D. Lawson, A.J. Ridley, Rho GTPase signaling complexes in cell migration and invasion, J. Cell Biol. 217 (2) (2018) 447–457, https://doi.org/10.1083/jcb.201612069.
[83] A.M. Murphy, D.J. Montell, Cell type-specific roles for Cdc42, Rac, and RhoL in Drosophila oogenesis, J. Cell Biol. 133 (3) (1996) 617–630.
[84] N. Colombie, V. Choesmel-Cadamuro, J. Series, G. Emery, X. Wang, D. Ramel, Non-autonomous role of Cdc42 in cell-cell communication during collective migration, Dev. Biol. (Basel) 423 (1) (2017) 12–18, https://doi.org/10.1016/j.ydbio.2017.01.018.
[85] A. Sahu, R. Ghosh, G. Deshpande, M. Prasad, A gap junction protein, Inx2, modulates calcium flux to specify border cell fate during Drosophila oogenesis, PLoS Genet. 13 (1) (2017) e1006542.10.1371/journal.pgen.1006542.
[86] H. Yue, B.A. Camley, W.J. Rappel, Minimal network topologies for signal processing during collective cell chemotaxis, Biophys. J. 114 (12) (2018) 2986–2999, https://doi.org/10.1016/j.bpj.2018.04.020.
[87] B.A. Camley, W.J. Rappel, Physical models of collective cell motility: from cell to tissue, J. Phys. D Appl. Phys. 50 (11) (2017), https://doi.org/10.1088/1361-6463/aa56fe.